

Positive Vibrational Entropy of Chemical Ordering in FeV

J. A. Muñoz,¹ M. S. Lucas,^{2,3} O. Delaire,² M. L. Winterrose,¹ L. Mauger,¹ Chen W. Li,¹ A. O. Sheets,³ M. B. Stone,²
D. L. Abernathy,² Yuming Xiao,⁴ Paul Chow,⁴ and B. Fultz¹

¹California Institute of Technology, W. M. Keck Laboratory 138-78, Pasadena, California 91125, USA

²Oak Ridge National Laboratory, 1 Bethel Valley Road, Oak Ridge, Tennessee 37831, USA

³Air Force Research Laboratory, Wright-Patterson AFB, Ohio 45433, USA

⁴HPCAT, Geophysical Laboratory, Carnegie Institution of Washington, Argonne, Illinois 60439, USA

(Received 11 December 2010; published 8 September 2011)

Inelastic neutron scattering and nuclear resonant inelastic x-ray scattering were used to measure phonon spectra of FeV as a *B2* ordered compound and as a bcc solid solution. The two data sets were combined to give an accurate phonon density of states, and the phonon partial densities of states for V and Fe atoms. Contrary to the behavior of ordering alloys studied to date, the phonons in the *B2* ordered phase are softer than in the solid solution. Ordering increases the vibrational entropy by $+0.22 \pm 0.03k_B$ /atom, which stabilizes the ordered phase to higher temperatures. First-principles calculations show that the number of electronic states at the Fermi level increases upon ordering, enhancing the screening between ions, and reducing the interatomic force constants. The effect of screening is larger at the V atomic sites than at the Fe atomic sites.

DOI: 10.1103/PhysRevLett.107.115501

PACS numbers: 63.20.dd, 63.20.kd, 64.60.Cn, 71.20.Be

At finite temperatures T , the entropy S of a material is dominated by the contribution from atom vibrations. Nevertheless, the relative stabilities of alloy phases depend on differences in their free energies, $F = E - TS$, and understanding differences in vibrational entropy is an active topic of research [1]. For chemical ordering transitions in alloys, the changes of vibrational entropy can be comparable to the large decrease in configurational entropy that accompanies ordering [2]. Stronger bonds between unlike pairs of atoms lead to ordering, and it is generally expected that such bonds would also be stiffer, reducing the vibrational entropy of the ordered phase [3]. For alloy systems that undergo chemical ordering, the decrease of vibrational entropy destabilizes the ordered phase with respect to the disordered phase [2,4–9]. To our knowledge, there are no experimental reports of an ordered phase that has a larger vibrational entropy than a disordered phase, but here we report that FeV is an exception and we show why.

The iron-vanadium alloy system has been investigated extensively, mainly because of its interesting magnetic behavior and chemical order-disorder phase transition. The phase diagram shows that bcc solid solutions are formed at high temperatures for all compositions, while the sigma phase is stable around the equiatomic composition [10,11]. The sigma phase can be avoided easily by quenching from high temperatures. Annealing at moderate temperatures results in *B2* order [12,13].

We report that the phonons in FeV become softer (shift to lower energies) upon ordering, so the *B2* ordered phase has a higher vibrational entropy than the disordered solid solution. First-principles calculations show how better electronic screening can cause a decrease of the average

energy of phonons in the ordered phase. At the Fermi energy, the projected electronic density of states (DOS) at the V atoms undergoes a larger increase with ordering than the projected DOS at the Fe atoms, and the phonon partial DOS of V shows a larger softening with ordering than the phonon partial DOS of Fe.

Samples were prepared by arc-melting vanadium slugs of 99.8% purity and iron lumps of 99.98% purity in equiatomic ratios under a high-purity argon atmosphere. For inelastic neutron scattering (INS) measurements, ingots of the arc-melted FeV, along with pieces of elemental iron and elemental vanadium, were cold rolled to a thickness of 1–2 mm, corresponding to a neutron scattering probability of 10%. The equiatomic alloy was annealed *in situ* during the experiment at 773 K for 8 hours under vacuum to induce *B2* ordering. The bulk and the shear moduli of the ordered and disordered samples were measured with ultrasonic pulse-echo instrumentation.

INS measurements were performed with the wide Angular-Range Chopper Spectrometer (ARCS) at the Spallation Neutron Source at the Oak Ridge National Laboratory. The nominal incident neutron energy was 80 meV. After subtracting the measured background, an iterative procedure that removes contributions from multiple scattering and higher order multiphonon processes was used to obtain the 1-phonon “neutron-weighted” density of states (NWDOS) curves [14,15]. The neutron weighting originates from the different efficiencies of Fe and V vibrations to scatter neutrons, proportional to their ratios of neutron cross section to mass, σ/M . The NWDOS curves (middle panel of Fig. 1) show significant softening after the alloy was annealed to develop *B2* order.

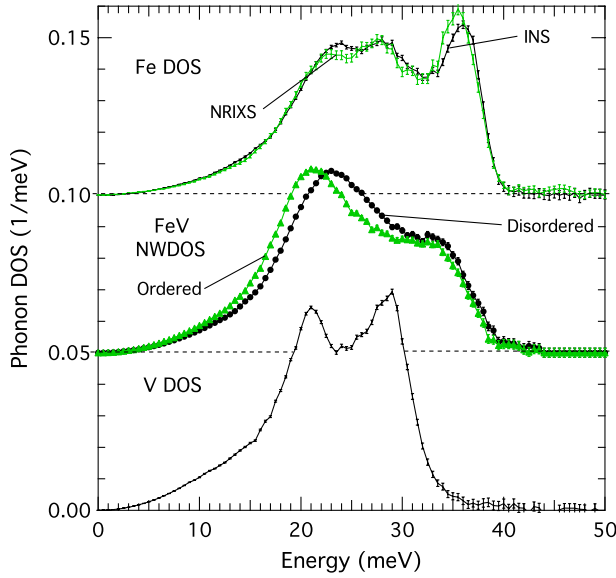


FIG. 1 (color online). Phonon DOS curves of pure Fe measured by INS and NRIXS (top panel). Neutron-weighted phonon DOS curves of FeV alloys (middle panel), and pure V (bottom panel) measured by INS. Error bars are from counting statistics.

The whole spectrum softens, but the low-energy modes are affected most.

Measurements of nuclear resonant inelastic x-ray scattering (NRIXS) were performed at beam line 16ID-D at the Advanced Photon Source at the Argonne National Laboratory on elemental ^{57}Fe and two ^{57}FeV samples with different degrees of $B2$ order. The alloys were 96.06% enriched with ^{57}Fe , were cold rolled to a thickness of 200 μm , and received the same heat treatment as the INS samples. The 1-phonon ^{57}Fe phonon partial DOS (pDOS) was calculated from the data using the standard program PHOENIX [16] and it is shown in the middle panel of Fig. 2. The NRIXS phonon DOS from pure bcc ^{57}Fe in the top panel of Fig. 1 is in excellent agreement with the INS result, especially considering the differences in the momentum transfer probed by the two methods.

A neutron-weight correction was made possible by combining the INS NWDOS spectra with the NRIXS Fe pDOS spectra [17]. The true phonon DOS is the concentration-weighted sum of the phonon pDOS curves of Fe and V, whereas the INS method gives the sum of these pDOS curves with the Fe pDOS 2 times stronger than for V owing to the difference in σ/M . Subtracting the excess weight of the Fe pDOS obtained from NRIXS gives the true phonon DOS, and subtracting all the Fe weight gives the V pDOS. The results are shown in the top and bottom panels of Fig. 2. The softening upon ordering in the V pDOS is larger than for the Fe pDOS.

The neutron scattering with energy transfers between -3 and 3 meV was used to obtain diffraction patterns. The intensities of the fundamental bcc diffraction peaks did not change after the *in situ* annealing to induce $B2$ order.

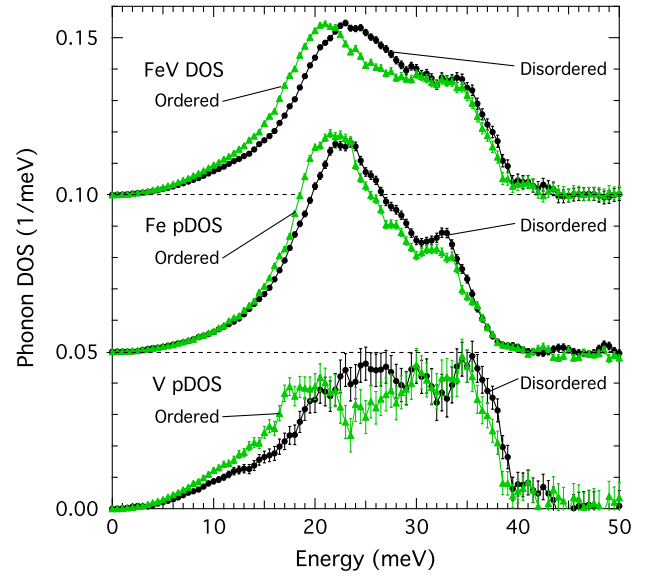


FIG. 2 (color online). Neutron-weight corrected phonon DOS curves of FeV samples (top panel), along with Fe pDOS curves (middle panel), and V pDOS curves (bottom panel). The Fe pDOS curves were determined directly by NRIXS measurements; the total FeV DOS curves and the V pDOS curves were obtained by combining INS and NRIXS spectra. Error bars are from counting statistics in the Fe pDOS, and propagation of error in the other curves.

The long-range order (LRO) parameter, L , was determined from the intensities of the superlattice diffraction peaks as in Ref. [18]. Results are listed in Table I.

The vibrational entropy per atom at a given temperature can be calculated from the phonon DOS measured at that temperature [1]. From the INS phonon DOS curves shown in Fig. 1, the vibrational entropy per atom was found to be $3.15 \pm 0.01 k_B$ in pure Fe and $3.64 \pm 0.01 k_B$ in pure V. The results for the FeV samples are given in Table I. The vibrational entropy of formation is $-0.07 \pm 0.02 k_B/\text{atom}$ for the disordered sample and $+0.07 \pm 0.02 k_B/\text{atom}$ for the ordered sample. For our samples with LRO parameters of 0.34 and 0.87, the vibrational entropy of ordering is $+0.14 \pm 0.02 k_B/\text{atom}$. From the change upon ordering of the V pDOS and the Fe pDOS, the V and Fe contributions to the vibrational entropy of ordering are $+0.16 \pm 0.05 k_B/\text{V atom}$, and $+0.08 \pm 0.02 k_B/\text{Fe atom}$. We can use the change in the LRO parameter upon ordering to obtain $\Delta S_{\text{vib}}^{A2 \rightarrow B2} = 0.22 \pm 0.03 k_B/\text{atom}$, the total change of vibrational entropy expected between states of full disorder and full order. In making this estimate, we assumed that the change in vibrational entropy scales with the fractional change of Fe-V bonds, and the total fraction of Fe-V bonds is $(1 + L^2)/2$. The same correction was used for the partial vibrational entropies for Fe and V atoms.

In binary systems with ordering tendencies, bonds between unlike atoms are more favorable energetically.

TABLE I. Values of the vibrational entropy per atom S_{vib} (k_B/atom) and average phonon energy $\langle E \rangle$ (meV), from neutron-weight corrected data for each sample and each atom species in FeV. The change in vibrational entropy, $\Delta S_{\text{vib}}^{A2 \rightarrow B2}$, is estimated for transition from full disorder ($A2$) to full $B2$ order. The values in parentheses are uncertainties in the last significant digit. Number of electronic states at the Fermi level \mathcal{N}_F (states/eV/atom) and magnetic moment M (μ_B) were calculated for the FeV alloy, and at the Fe and V sites, from first-principles for the SQS and $B2$ structure. Lower rows are long-range order parameter L , lattice parameter a , shear modulus G , and bulk modulus B , for the disordered (SQS) and ordered ($B2$) samples.

	Disordered		Ordered		Transition $\Delta S_{\text{vib}}^{A2 \rightarrow B2}$	SQS		$B2$	
	S_{vib}	$\langle E \rangle$	S_{vib}	$\langle E \rangle$		\mathcal{N}_F	M	\mathcal{N}_F	M
FeV	3.33(2)	25.1(2)	3.47(2)	24.2(2)	0.22(3)	1.66	0.62	2.67	0.40
Fe atom	3.44(1)	24.2(1)	3.52(1)	23.6(1)	0.12(3)	0.76	1.67	1.18	1.16
V atom	3.24(4)	26.0(4)	3.40(4)	24.8(4)	0.25(8)	0.80	-0.39	1.50	-0.33
L	0.34		0.87			0.00		1.00	
a	2.938(2) Å		2.931(3) Å			2.938 Å		2.870 Å	
G	74.4(5) GPa		65.6(5) GPa			76.4 GPa		68.7 GPa	
B	161(5) GPa		176(5) GPa			182 GPa		195 GPa	

In measurements on other alloy systems that develop order (see Refs. [1,19] for compendia), it has been observed that bonds between unlike atoms are also stiffer than bonds between like atoms, so the vibrational entropy is lower in the ordered phase. This behavior is consistent with a Lennard-Jones potential, for example, where stronger bonds are stiffer bonds, the ordered phase has a lower vibrational entropy, and the critical temperature of the ordering transition is suppressed [3]. Prior *ab initio* computational work showed that with a change in structure of the parent lattice, ordered compounds may have soft phonons and large vibrational entropies [20]. A larger vibrational entropy in a DO_{22} -ordered phase in Pd_3V was attributed to lattice relaxation effects in the noncubic structure [21]. To our knowledge, phonon softening with chemical ordering has not been reported in any previous experimental work for any systems in which there is no change in symmetry of the underlying parent lattice.

The electronic DOS was calculated from first-principles using density functional theory. The bcc solid solution was simulated with a special quasirandom structure (SQS), a specially-designed periodic structure with the same values of atomic correlation functions (in the cluster expansion formalism [22]) as the random solid solution [23]. We used the 16-atom SQS for the bcc structure published by Jiang *et al.* [24]. The spin-polarized calculations used VASP [25] with the projector-augmented wave method [26] and the generalized gradient approximation [27]. The k -point meshes for Brillouin zone sampling were constructed using the Monkhorst-Pack scheme [28]. The volumes of both structures were optimized, and convergence with respect to the kinetic energy cutoff and the sampling of k points in the Brillouin zone was achieved. The total number of k points times the total number of atoms per unit cell was 8192 for both the SQS and $B2$ structure. The plane wave cutoff energy was 420 eV. The calculations predict the $B2$ ordered structure to be more stable than the SQS, with ground state energies of -17.498 eV/unit cell and

-17.462 eV/unit cell, respectively. The trends in the calculated lattice parameters and elastic moduli were in good agreement with experimental data (Table I). The bulk modulus stiffens upon ordering, which is the usual behavior in ordering systems. Nevertheless, the shear modulus decreases, showing that transverse and longitudinal modes respond differently to ordering and suggesting that the transverse modes are mainly responsible for the observed softening.

The spin-polarized electronic DOS curves of the SQS and $B2$ structure are shown in Fig. 3, along with the calculations of Johnson *et al.* [29] performed using the coherent-potential approximation (CPA) mean field theory to average over the chemical disorder. We found a considerable increase in the number of electronic states at the Fermi level (\mathcal{N}_F) upon ordering, from 1.66 to 2.67 states/eV/unit cell. The electronic states near the Fermi level are available for screening the displacements of the ions, and changes in screening can have important

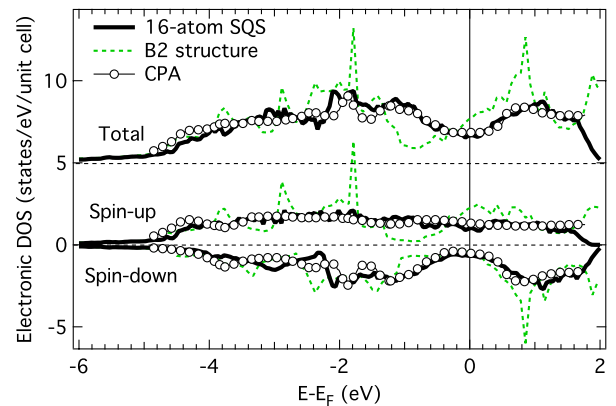


FIG. 3 (color online). Spin-polarized electronic DOS computed from first-principles with VASP for equiatomic FeV in the $B2$ structure, and in a 16-atom SQS. Calculations performed by Johnson *et al.* [29] using a CPA method are included for comparison. The total eDOS is offset for clarity.

consequences on the phonon DOS [30–33]. In equiatomic FeV, this increase in \mathcal{N}_F is consistent with more ionic screening and softer interatomic forces, as observed experimentally. Preliminary calculations of the intraband generalized susceptibility [34] were performed for the majority spin bands near the Fermi surface. Along high symmetry directions we found the generalized susceptibility was consistently 2.5 times larger for the ordered B2 structure than for a 2-atom SQS, in good agreement with the change in \mathcal{N}_F for the same structures. The charge transferred to the Fe atoms from V atoms upon ordering is small ($0.08e^-$ /atom), and its expected effect of stiffening the bonds is also small.

Different phonon polarizations respond differently to chemical order. As shown in Fig. 2, low-energy phonons (below 30 meV), which represent mostly transverse modes, show the largest softening. The high energy phonons are mostly longitudinal and soften considerably less. This contrast is consistent with the measured and calculated elastic moduli, which shows the behavior of the transverse and longitudinal modes in the long wave length limit. The behavior of the phonons in the Fe and V phonon pDOS curves respond to chemical order in a similar way. Nevertheless, the effect is larger for the pDOS of V atoms, which softens more upon ordering than the Fe pDOS, with the decrease in average phonon energy being twice as large for V as for Fe. Interestingly, the projection of \mathcal{N}_F onto V atoms increases with ordering by a factor of 1.7 more than for Fe atoms. This suggests that screening of the displacements of V atoms may be more effective than for Fe atoms, consistent with the observed behavior of the phonon pDOS. Correlations have been reported previously between the total electron DOS at the Fermi level and softening of the total phonon DOS. This new correlation between the projected electronic DOS at an atom and the softening of its partial phonon DOS may be more general, but needs further corroboration.

We thank M. Loguillo for technical support on the ARCS instrument. This work was supported by the Department of Energy through the Basic Energy Sciences Grant DE-FG02-03ER46055. The portions of this work conducted at Oak Ridge National Laboratory were supported by the Scientific User Facilities Division and by the Division of Materials Sciences and Engineering, Office of Basic Energy Sciences, DOE. Portions of this work were performed at HPCAT (Sector 16), Advanced Photon Source (APS), Argonne National Laboratory. HPCAT is supported by CIW, CDAC, UNLV and LLNL through funding from DOE-NNSA, DOE-BES and NSF. APS is supported by DOE-BES, under Contract No. DE-AC02-06CH11357. This work benefited from DANSE software developed under NSF Grant No. DMR-0520547.

- [1] B. Fultz, *Prog. Mater. Sci.* **55**, 247 (2010).
- [2] L. Anthony, J. K. Okamoto, and B. Fultz, *Phys. Rev. Lett.* **70**, 1128 (1993).
- [3] G. D. Garbulsky and G. Ceder, *Phys. Rev. B* **53**, 8993 (1996).
- [4] L. Anthony, L. J. Nagel, J. K. Okamoto, and B. Fultz, *Phys. Rev. Lett.* **73**, 3034 (1994).
- [5] B. Fultz *et al.*, *Phys. Rev. B* **52**, 3280 (1995).
- [6] B. Fultz *et al.*, *Phys. Rev. B* **52**, 3315 (1995).
- [7] L. J. Nagel, L. Anthony, and B. Fultz, *Philos. Mag. Lett.* **72**, 421 (1995).
- [8] L. J. Nagel, B. Fultz, J. L. Robertson, and S. Spooner, *Phys. Rev. B* **55**, 2903 (1997).
- [9] M. S. Lucas *et al.*, *J. Appl. Phys.* **108**, 023519 (2010).
- [10] *Smithells Metals Reference Book* edited by E. A. Brandes and G. B. Brook (Butterworth-Heinemann, Ltd., Jordan Hill, Oxford, 1992) p. 11.
- [11] J. O. Andersson, *CALPHAD: Comput. Coupling Phase Diagrams Thermochem.* **7**, 305 (1983).
- [12] J. I. Seki, M. Hagiwara, and T. Suzuki, *J. Mater. Sci.* **14**, 2404 (1979).
- [13] J. M. Sanchez, M. C. Cadeville, V. Pierron-Bohnes, and G. Inden, *Phys. Rev. B* **54**, 8958 (1996).
- [14] M. Kresch *et al.*, *Phys. Rev. B* **75**, 104301 (2007).
- [15] B. Fultz *et al.*, <http://docs.danse.us/DrChops/ExperimentalInelasticNeutronScattering.pdf>.
- [16] W. Sturhahn, *Hyperfine Interact.* **125**, 149 (2000).
- [17] M. S. Lucas *et al.*, *Phys. Rev. B* **82**, 144306 (2010).
- [18] T. Ziller *et al.*, *Phys. Rev. B* **65**, 024204 (2001).
- [19] A. van de Walle and G. Ceder, *Rev. Mod. Phys.* **74**, 11 (2002).
- [20] C. Wolverton and V. Ozolins, *Phys. Rev. Lett.* **86**, 5518 (2001).
- [21] A. van de Walle and G. Ceder, *Phys. Rev. B* **61**, 5972 (2000).
- [22] R. Kikuchi, *Phys. Rev.* **81**, 988 (1951); J. M. Sanchez, F. Ducastelle, and D. Gratias, *Physica (Amsterdam)* **128A**, 334 (1984).
- [23] A. Zunger, S.-H. Wei, L. G. Ferreira, and J. E. Bernard, *Phys. Rev. Lett.* **65**, 353 (1990).
- [24] C. Jiang *et al.*, *Phys. Rev. B* **69**, 214202 (2004).
- [25] G. Kresse and J. Furthmüller, *Phys. Rev. B* **54**, 11169 (1996); *Comput. Mater. Sci.* **6**, 15 (1996).
- [26] P. E. Blöchl, *Phys. Rev. B* **50**, 17953 (1994); G. Kresse and D. Joubert *ibid.* **59**, 1758 (1999).
- [27] J. P. Perdew, K. Burke, and M. Ernzerhof, *Phys. Rev. Lett.* **77**, 3865 (1996).
- [28] H. J. Monkhorst and J. D. Pack, *Phys. Rev. B* **13**, 5188 (1976).
- [29] D. D. Johnson, F. J. Pinski, and J. B. Staunton, *J. Appl. Phys.* **61**, 3715 (1987).
- [30] O. Delaire and B. Fultz, *Phys. Rev. Lett.* **97**, 245701 (2006).
- [31] O. Delaire *et al.*, *Phys. Rev. B* **77**, 214112 (2008).
- [32] O. Delaire *et al.*, *Phys. Rev. Lett.* **101**, 105504 (2008).
- [33] O. Delaire *et al.*, *Proc. Natl. Acad. Sci. U.S.A.* **108**, 4725 (2011).
- [34] J. Rath and A. J. Freeman, *Phys. Rev. B* **11**, 2109 (1975).